Biology Direct

RESEARCH

Open Access

A comprehensive molecular characterization of a claudin-low luminal B breast tumor

Sara Giovannini[1†], Artem Smirnov[1,2†], Livia Concetti[1†], Manuel Scimeca[1], Alessandro Mauriello[1], Julia Bischof[3], Valentina Rovella[1], Gerry Melino[1], Claudio Oreste Buonomo[1*], Eleonora Candi[1,2*] and Francesca Bernassola[1*]

Abstract

Breast cancer is the most common cause of death from cancer in women. Here, we present the case of a 43-year-old woman, who received a diagnosis of claudin-low luminal B breast cancer. The lesion revealed to be a poorly differentiated high-grade infiltrating ductal carcinoma, which was strongly estrogen receptor (ER)/progesterone receptor (PR) positive and human epidermal growth factor receptor (HER2) negative. Her tumor underwent in-depth chromosomal, mutational and gene expression analyses. We found a pathogenic protein truncating mutation in the *TP53* gene, which is predicted to disrupt its transcriptional activity. The patient also harbors germline mutations in some mismatch repair (MMR) genes, and her tumor displays the presence of immune infiltrates, high tumor mutational burden (TMB) status and the apolipoprotein B mRNA editing enzyme catalytic polypeptide 3 (APOBEC3) associated signatures, which, overall, are predictive for the use of immunotherapy. Here, we propose promising prognostic indicators as well as potential therapeutic strategies based on the molecular characterization of the tumor.

Keywords Luminal breast cancer, Claudin-low tumors

Introduction

Breast cancer, the most common cancer in women worldwide, represents a genetically, histologically, and clinically heterogeneous disease with multiple distinct subtypes [1–6]. These subtypes are commonly defined based on the immunohistochemical detection of estrogen receptor (ER), progesterone receptor (PR) and human epidermal growth factor receptor (HER2). Breast cancer can be classified into five main molecular subtypes [7–10]. Luminal A breast cancers are HER2-negative with low levels of proliferation (Ki-67 < 20%) but show ER and/or PR positivity. Therefore, these cases are clinically slow growing and low grade and are associated with the best survival rate and lowest relapse incidence. Luminal B cases, similarly, are also ER^{pos}, $PR^{low/neg}$ $HER2^{neg}$, but show a much high expression of Ki67 (> 20%; https://www.ncbi.nlm.nih.gov/books/NBK583808/) [11–14]. They are intermediate/high histologic grade, grow faster than luminal A tumors and correlate with less favorable prognosis. The HER2 subtype is characterized by high expression of HER2 and variable expression of ER, PR and Ki67 [15]. The luminal HER2 subtype is defined by ER/PR positivity with 15–30% of Ki-67 expressing cells, while the HER2-enriched sub-group is ER^{neg}/PR^{neg} and displays higher Ki-67 positivity (> 30%). The HER2

[†]Sara Giovannini, Artem Smirnov and Livia Concetti equally contributed to this work.

*Correspondence:
Claudio Oreste Buonomo
o.buonomo@inwind.it
Eleonora Candi
candi@uniroma2.it
Francesca Bernassola
bernasso@uniroma2.it
[1] Department of Experimental Medicine, TOR, University of Rome Tor Vergata, 00133 Rome, Italy
[2] Istituto Dermopatico Immacolata (IDI-IRCCS), 00100 Rome, Italy
[3] Germany Biochemistry Laboratory, Indivumed GmbH, Falkenried, 88 Building D, 20251 Hamburg, Germany

subtype is fast-growing and is generally more aggressive, with a worse outcome compared to luminal cancers, although prognosis has been improved by the introduction of HER2-targeted therapies. The last subgroup is the triple negative breast cancer (TNBC), which is negative for all hormone receptors as well as for HER2 expression [16, 17]. It is poorly differentiated, highly proliferative, and it is associated with the most adverse prognosis. Further sub-classification of breast tumors into new molecular entities allowed the identification of distinct sub-type, such as the claudin-low [12, 18–20]. Clinically, claudin-low tumors show a poor prognosis with invasive ductal carcinomas that preferentially, but not exclusively, display a TNBC phenotype [21]. They are typically associated with young age of onset, high tumor grade, large tumor size, local recurrence rate and massive lymphocytic infiltrate within the tumor microenvironment [22, 23]. Claudin-low tumors generally exhibit high levels of genomic instability.

Endocrine therapy represents the standard treatment for hormone receptor positive breast cancers and has increased the overall prognosis of the luminal subtype. Nevertheless, most patients, eventually develop resistance to endocrine therapy, thus limiting their efficacy. Acquired endocrine resistance mechanisms in hormone receptor-positive breast tumors include the occurrence of somatic mutations leading to the activation of signaling pathways that can bypass estrogen dependency. Somatic mutations associated with endocrine resistance comprise *EGFR* amplification and activation of the insulin/IGF-I receptor pathway [24, 25].

In this case report, we present a luminal B breast cancer patient, with high cancer proliferation features. A molecular profiling of the tumor was achieved by exploiting genome-wide mutational analyses, transcriptomics, the tumor mutational burden (TMB) rate, microsatellite instability (MSI), immune checkpoints, and cancer mutational signatures.

Case presentation

Case narration

Here we report the case of a 43-years old woman who underwent surgery in 2020 for a malignant nodule (diameter of 1.2 cm) in the lower inner quadrant of the left breast (Table 1). According to the Nottingham grading system [26], breast lesions have been classified as a poorly differentiated high-grade infiltrating ductal carcinoma (G3; tubules 3; pleomorphism 3; mitosis 2). No metastatic cells were observed in the sentinel lymph node. The TNM staging was pT1c, N0. Immunohistochemical analysis allowed for classification of the breast lesions as luminal B breast cancer. Specifically, the histology showed high positivity for both ER (80% positive cells) and PR (60% positive cells), a high proliferation index (ki67 = 35%) and c-Erb-B2 score 1 (Fig. 1A–D). The expression levels of ER1 (medium), PR (high) and HER2 (low) and MKI67 (high) were also confirmed by RNA-seq analysis. As shown in Fig. 1E, the patient indeed showed upregulation of ER1/PR1, very weak expression of HER2 and elevated levels of MKI67 as compared to the clinical cohort (316 $ER^{pos}PR^{pos}HER2^{neg}$ cases out of total 586 breast cancer patients). The diagnosis of luminal B subtype was consistent with both histopathological and molecular data.

Further characterization of the patient specimen by gene expression profiling classified the tumor as a

Table 1 Clinical data of the breast cancer patient enrolled in this study

Parameters	Description
Gender	Female
Age at surgery	47
Smoker	Yes
Tumor type	Breast primary tumor
Histological type	Ductal carcinoma
Subtype	Luminal B Claudin (ER + PR + HER2−)
TNM	T1c N0 M0
ICD	C50.3
Grading	G3
Dignity	Malignant
Ki-67	35
Treatment	Surgery (2020–10–27)
Therapy	CHT adj (Adriamycin A + Cyclophosphamide AC) + PTX (Paclitaxel) + hormone therapy HRH (enanthone) + exemestane and RDT.mammography total body scan negative

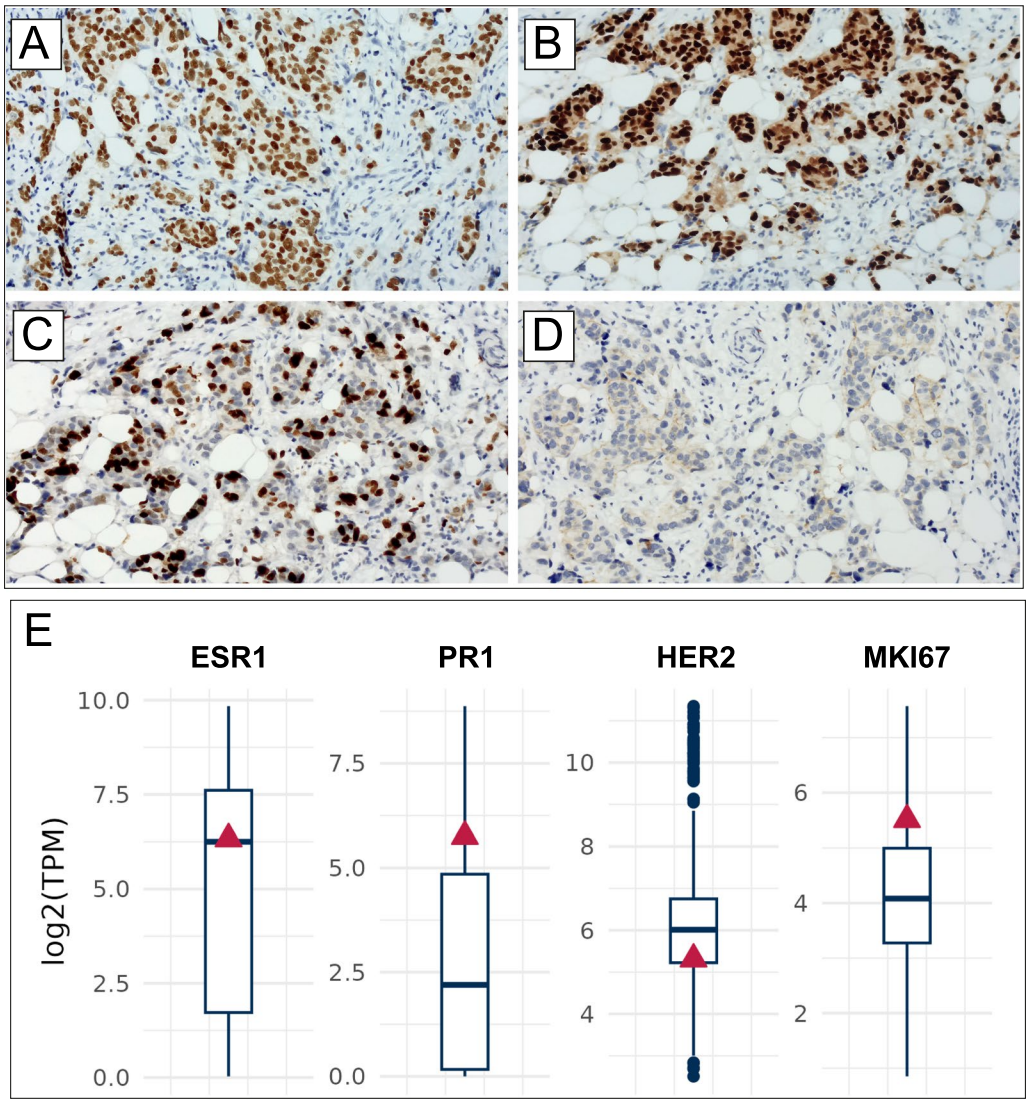

Fig. 1 Histological and immunohistochemical evaluation and the molecular profile of a breast carcinoma. Images shows **A** high percentage of ER positive cancer cells in a poorly differentiated high-grade infiltrating ductal carcinoma, **B** numerous PR positive breast cancer cells, **C** Ki67 staining displaying a high proliferation index, **D** very low c-Erb-B2 expression in breast infiltrating cancer cells (c-Erb-B2 score 1). **E** RNA-Seq expression levels (TPM) of ER1 (ER1, ESR1), PR 1 (PR1), HER2 and proliferation marker Ki-67 (MKI67) for the patient (red triangle) and the clinical cohort (blue boxplot)

claudin-low breast cancer. Claudin-low tumors are characterized by a specific gene expression profile, which includes low expression of genes associated with tight junctions and epithelial cell–cell adhesion, including claudins (CLDNs) 3, 4 and 7 [21, 22]. They are typically, but not exclusively negative for ER, PR, and HER2 [22]. Claudin-low tumors can be either enriched in mesenchymal traits or in stem cell features depending on the specific subgroup [27]; they also display high immune cell infiltration and low luminal/epithelial differentiation [28]. In agreement with a mesenchymal/stem cell-like state, claudin-low tumors are characterized by high expression of vimentin and N-cadherin, and several transcriptional repressors of E-cadherin [18, 28, 29]. As shown in Fig. 2A, the tumor showed downregulation of CLDN1, CLDN4, CLDN7 and CLDN8, relatively to the non-claudin low cohort. Coherently, low expression of claudins (Fig. 2A) in the patient correlated with elevated mRNA levels of the CDH2 gene encoding N-cadherin (Fig. 2B) and of transcriptional repressors of E-cadherin, such as the epithelial-mesenchymal transition (EMT)-inducing transcriptional factors SNAI1, SNAI2, TWIST1, TWIST2, ZEB1 and ZEB2 (Fig. 2C). In addition, we observed high expression of other EMT-inducing factors, including HIF1α (Fig. 2D), and high EMT and hypoxia related expression signature scores (Fig. 2E). The

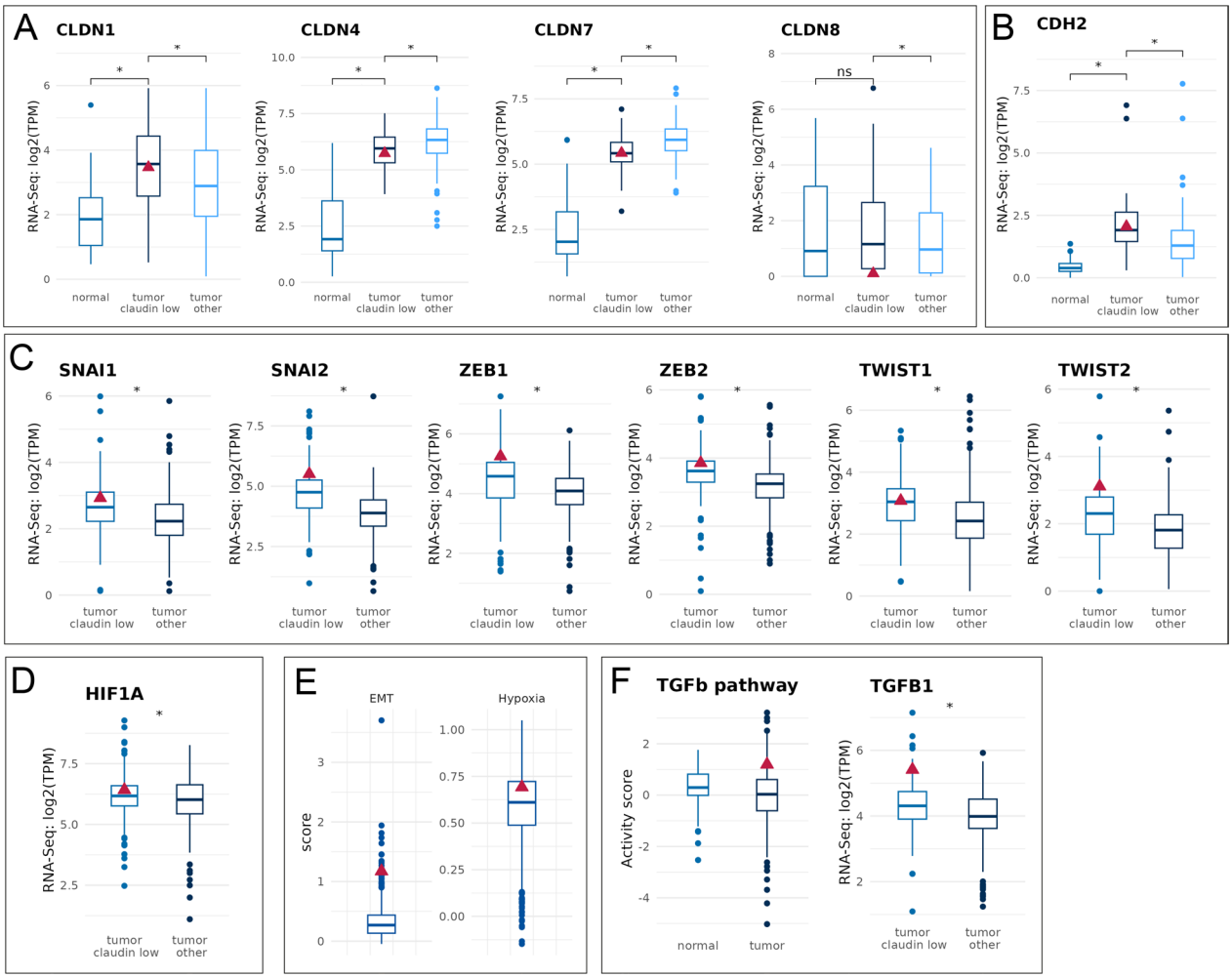

Fig. 2 Molecular alterations detected in the patient. **A** RNA-Seq expression levels of CLDN1, CLDN4, CLDN7 and CLDN8 in the patient relatively to the non-claudin low cohort. **B** CHD2 (N-cadherin) is highly expressed in the patient relatively to the claudin low tumor group as well as to the non-claudin low cohort. **C** RNA-Seq expression levels of EMT-inducing transcriptional factors (where low values refer to epithelial cell status and high values to mesenchymal cells), and **D** HIF1α. **E** EMT and hypoxia expression signature scores assessed in the tumor. Hypoxia is measured as frequency between 0 and 1. EMT score represents epithelial like as low score and mesenchymal like as high scores. **F** TGF-β pathway activity score relatively to the normal tissue and RNA-Seq expression levels of TGF-β1

TGF-β signaling promotes breast cancer invasion and metastasis by driving EMT through transcriptional regulation of EMT factors, such as SNAIL, SLUG and TWIST [30, 31]. Approximately 40% of human breast tumors display a positive TGF-β gene response signature that is more associated with in ER^{neg} tumors and lung metastasis [32]. In this regard, the patient showed a relatively high TGF-β pathway activity score as compared to normal tissue along with elevated of TGF-β1 expression relatively to the clinical cohort (Fig. 2F). Claudin-low tumors are also characterized by marked immune and stromal cell infiltration [27]. Immunohistochemical evaluation of the tumor revealed the presence of immune cell infiltration (Fig. 3A and B). Additionally, gene expression analyses confirmed that the tumor was highly infiltrated by immune cells including cytotoxic lymphocytes, NK, T and CD8+ T cells relatively to the clinical cohort (Fig. 3C).

Breast cancer is characterized by genomic complexity with different chromosomal and gene alterations, with the most frequently altered genes being *BRCA1/2*, *TP53*, *PTEN*, *PIK3CA*, *ERBB2*, *FGFR1*, *CCND1*, *BARD1* and *PALB2* [33, 34]. Breast cancer is generally driven by multiple mutations at low penetrance that act cumulatively. Luminal/ER-positive subtypes are reported to be the most heterogeneous in terms of mutation spectrum and copy number changes [35]. A comprehensive genomic profiling of the tumor indicated the presence

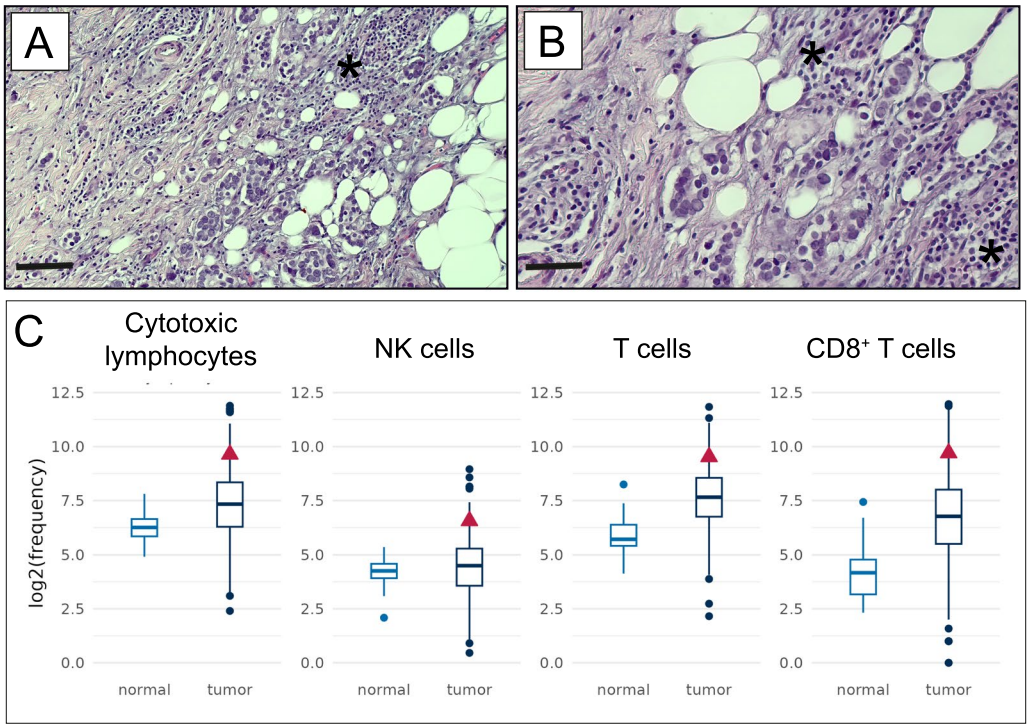

Fig. 3 Presence of immune infiltrates in the tumor. **A** Intertumoral inflammatory infiltrate (asterisk) in an infiltrating breast carcinoma. **B** High magnification of panel A displaying lymphocyte intertumoral infiltrates (asterisks). Scale bar represents 50 µm for panel A and 100 µm for panel B. **C** Immune cell deconvolution. High immune cells infiltration in the patient, represented by high frequencies of cytotoxic lymphocytes, T cells (specifically CD8 +) and NK cells

of three concurrent somatic mutations with single base substitutions in the epidermal growth factor receptor (*EGFR*), insulin growth factor receptor-1 (*IGF1R*) and *TP53* genes (Table 2 and Fig. 3), which are mutated in several aggressive tumors [36–42]. Activated EGFR is a well-known therapeutic target in lung and breast cancer, in which small molecule tyrosine kinase inhibitors or anti-EGFR monoclonal antibodies can be exploited [43]. Nevertheless, the single nucleotide variant c.844G>A (p.Glu282Lys) of the gene encoding the EGFR identified in the patient (Fig. 4A), and previously reported in lung cancer, it is unlikely to be pathogenetic and was not found in both the METABRIC [44] and TCGA [34] datasets in cBioPortal [45].

We identified a somatic mutation c.3187-5C>T (p.Met186Val) in the I*GF1R* gene that was also found in one out of 3593 METABRIC/TCGA patients. However, this variant had never been described in mammary tumors or in other cancer types, therefore its clinical significance remains unknown. This mutation is located within the L1 domain of the IGF1-binding site (Fig. 4B) in the IGF1 protein and is predicted to alter a non-conserved nucleotide, which is close to a canonical splice site. Whether and how the mutation could affect mRNA splicing needs to be elucidated. In addition, IGF1R gene amplification was detected in the patient (Fig. 4C and Table 2). IGF1R controls the expression of genes that regulate cell survival and cell cycle progression, thus critically influencing tumorigenesis. Gene amplification or overexpression of IGF1R are frequent events across several tumor types, including breast cancer, though activating mutations of the *IGF-1R* gene have not been reported [46]. Accordingly, no *IGF1R* mutations were found in the METABRIC/TCGA datasets. Overall, at least 50% of breast tumors have an activated IGF-1R [47] that has been reported to play a crucial role in cancer promotion [48]. However, opposing evidence also exists, supporting the possibility that the IGF-1R has a dual function in cancer, and can also act as a tumor suppressor. More recent reports have indeed indicated that overexpression of IGF-1R in luminal breast cancers is associated with a favorable prognosis, with low expression of IGF1R resulting in a more undifferentiated tumor phenotype and worse outcome [47, 49].

The c.637C>T (p.Arg213stop) variant of *TP53* is a protein truncating mutation that lies within the DNA binding domain (Fig. 4D) and is reported to be a pathogenic mutation [50]. It has been previously identified in breast cancer patients [51]. According to the METABRIC/TCGA datasets, this variant of TP53 is found in 0,7% of

Table 2 Genetic alterations detected in the tumor

Gene		Somatic variations	Nucleotide change	Amino acid change
EGFR		Neutral mutation	c.844G>A	Glu282Lys
IGF1R		Unknown mutation	c.3187-5C>T	Met186Val
TP53		Truncating mutation	c.637C>T	Arg213stop
Gene		**Gene amplifications**		
CHD2				
IGF1R				
Gene	**System**	**Germline variations**		**Nt or AA change**
CHEK1	Damage signaling/Checkpoint	Missense variant		Ile377Val
ERCC2	NER	Missense variant		Asp19Asn
ERCC4		Splice region variant and intron variant		947-7G>A
ERCC5		Missense variant		Gly1053Arg
ERCC6		Splice region variant and intron variant		1821+7C>T
FANCI	FA	Missense variant		Ala 86Val
MSH2	MMR	Splice region variant and intron variant	c.2006-6T>C	2006-6T>C
MSH3		Conservative in frame insertion	181_189dup	Ala61_Pro63dup
MSH6		Missense variant	c.116G>A	Gly39Glu
PMS2		Splice region variant and intron variant	c.706-4delT	706-4delT
TP53BP1	NHEJ	Missense variant		Asp353Glu
BARD1	HR	Splice region variant		*481dupA
PALB2		Missense variant	c.791A>T	Gln264Arg
EME1		Missense variant		Glu69Asp
TOP3A		Splice region variant and non-coding transcript exon variant		599_600dupAA
POLE	TLS/BER/NER/HR	Missense variant		Arg1259His
POLQ	TLS/HR/ALT-NHEJ/TMEJ	Missense variant		Thr1151Ala

Nucleotide changes are reported only for potential clinically relevant mutations. EGFR, epidermal growth factor receptor; IGF1R, Insulin-like growth factor 1 receptor; TP53, Tumor protein p53 gene; CHD2, Chromodomain Helicase DNA Binding Protein 2; CHEK1, Checkpoint Kinase 1; ERCC2, ERCC excision repair 2, TFIIH core complex helicase subunit; ERCC4, ERCC excision repair 4, endonuclease catalytic subunit; ERCC5, ERCC excision repair 5, endonuclease; ERCC6, ERCC excision repair 6, chromatin remodeling factor; FANCI, FA complementation group I; MSH2, mutS homolog 2; MSH3, mutS homolog 3; MSH6, mutS homolog 6; PMS1 homolog 2, mismatch repair system component; tumor protein p53 binding protein 1; BARD1, BRCA1 associated RING domain 1; PALB2, partner and localizer of BRCA2; EME1, essential meiotic structure-specific endonuclease 1; TOP3A, DNA topoisomerase III alpha; POLE, DNA polymerase epsilon, catalytic subunit; POLQ, DNA polymerase theta; NER, Nucleotide excision repair; FA, Fanconi anemia; MMR, Mismatch repair; NHEJ, Non-homologous end joining; HR, Homologous recombination; TLS, Translesion DNA synthesis; BER, Base excision eepair; ALT-NHEJ, Alternative-NHEJ; TMEJ, polymerase theta-mediated end-joining

breast cancer cases. Interestingly, the combination of temozolomide and PARP inhibitors treatment increases DNA double-strand breaks and results in augmented cytotoxicity in breast and lung cancer patient-derived tumor organoids bearing the p.Arg213stop variant of *TP53* [51].

Among the amplified genes, we also found chromodomain helicase DNA-binding protein 2 (*CHD2* (Fig. 4E and Table 2). There is some evidence that CHD2 has a role in cancer. It has been proposed to prevent breast cancer [52], while divergent evidence highlighted the presence of inactivating mutations in the CHD2 gene that have been associated with increased susceptibility to tumor development [53]. To our knowledge, amplification of *CHD2* has not been previously described in breast cancer patients and its biological relevance remains unexplored. The analysis of the METABRIC/TCGA and datasets revealed that both *CHD2* and *IGF1R* genes are amplified in 3% of breast cancer patients. Because they lie in proximity on chromosome 15, they are also co-amplified in 2.3% of cases, independently from TP53 or EGFR alterations (Fig. 4F).

The patient also harbors germline variations in several DNA damage repair (DDR) genes (Table 2), with the homologous recombination (HR, mutations in 4/21 tested HR-related genes), the mismatch (MMR, mutations in 4/10 tested MMR-related genes) and the nucleotide excision (NER, 4/10 tested NER-related genes) repair systems being the most affected. Genetic susceptibility to breast cancer is known to be determined

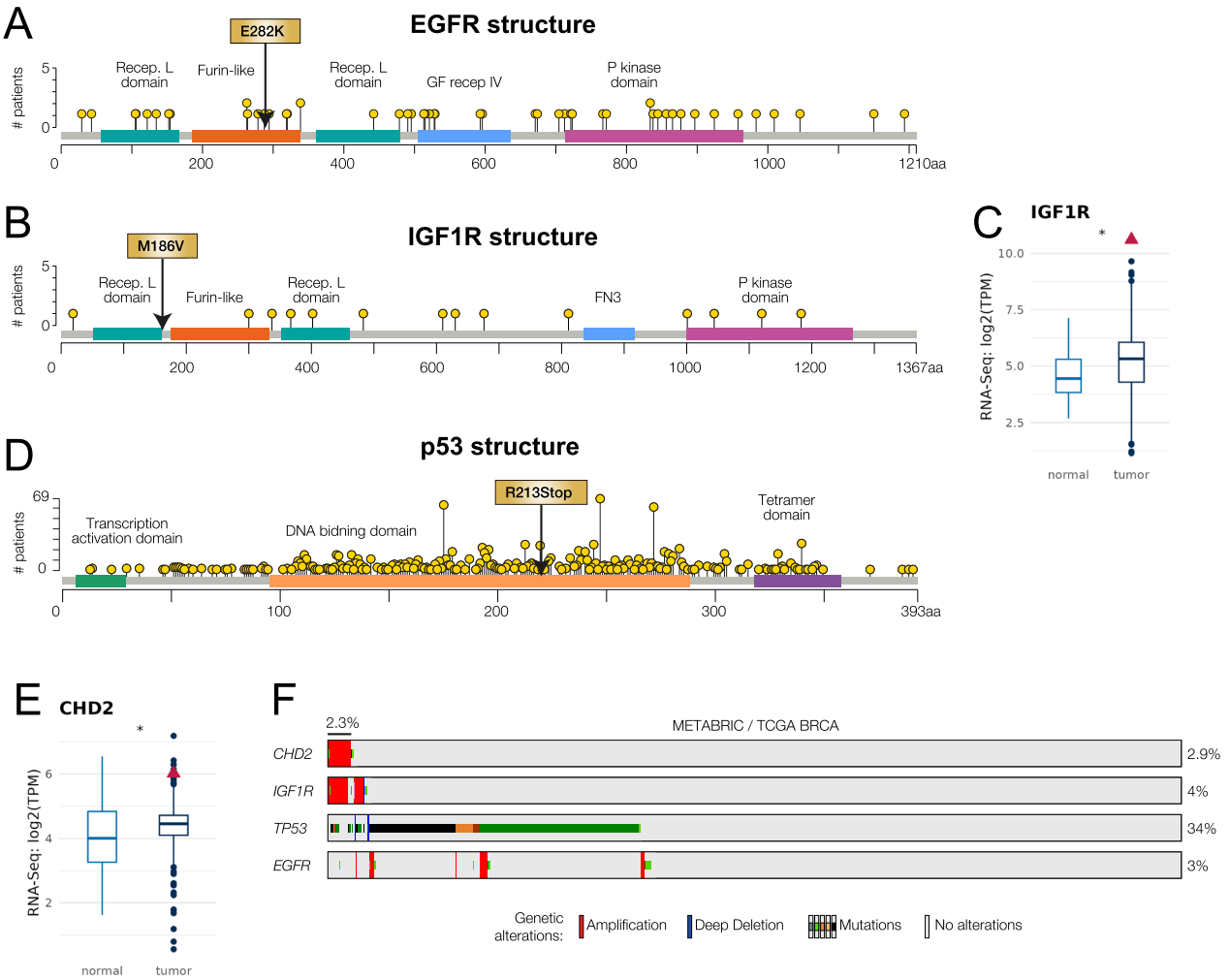

Fig. 4 Molecular and chromosomal alterations detected in the breast cancer patient. Schematic structural features of **A** EGFR, **B** IGF1R, and **D** p53 proteins as well as mutations observed in the METABRIC and TCGA datasets. The mutations observed in both the METABRIC and TCGA-BRCA datasets and in the patient of this case study are highlighted with lollipop plots and were exported from cBioPortal. Patient's mutations are indicated by an arrow. Data were obtained from cBioPortal. **C**, **E** IGF1R and CHD2 gene amplifications in the patient relatively to the clinical cohort. **F** *CHD2*, *EGFR*, *IGF1R*, and *TP53* genomic alterations in the METABRIC and TCGA-BRCA datasets as an OncoPrint plot. The plots were exported from cBioPortal

by common variants along with the occurrence of rare mutations conferring higher disease risks. The latter comprises missense mutations and protein-truncating variants in the following genes: *TP53, BRCA1/2, ATM, PALB2*, *BARD1, CHEK2*, and *RAD51* [54]. Here, we identified heterozygous germline variants of the *MSH2*, *MSH3*, *MSH6* and *PMS2* genes (Table 2). Of note, the nucleotide variant c.2006-6T>C in the *MSH2* gene (intron variant) has been associated with an increased risk of non-Hodgkin's lymphomas and other hematological malignancies [55]. In addition, the 2006-6T>C variant in *MSH2* has been detected in a male breast cancer patient, though the biological significance has not been established yet. The 181_189dup variant (Ala61_Pro63dup) of the *MSH3* gene has been previously reported in a patient with breast cancer, though it has been classified as a polymorphism variant [56]. We also detected the c.116G>A missense mutation in the *MSH6* gene leading to the substitution of a glutamic acid for glycine at position 39 (p.Gly39Glu) of the MSH6 N-terminal region. This variant has been previously described in thyroid cancer patients although the functional outcome of this mutation has been only speculated [57]. Santos and collaborators [57]) have proposed that because the mutation is positioned near two phosphorylation sites (Ser41 and Ser43) located

within a nuclear localization sequence and targeted by MAPKs, it is possible that it interferes with the modification of these residues, ultimately influencing the stability, the nuclear import, or the biological function of MSH6. Since glutamate is a negatively charged residue, the authors also speculated that the p.Gly39Glu substitution could alter the ability of MSH6 to bind DNA and, as a result, its DNA repairing capacity. Finally, the *PMS2* c.706-4delT mutation (intron variant) has been observed in a patient diagnosed with Lynch syndrome and in a subject affected by ovarian carcinoma [58]. It is a splice variant that has been classified as benign. The patient also harbors a missense variant c.791A>T in the PALB2 gene (Gln264Arg) and a splicing variant in the BARD1 gene. To our knowledge, these mutations have not been described in other cancer patients and their biological relevance remains unknown.

Since the DNA repair cellular systems are indispensable for the maintenance of the genomic fidelity and for reducing general gene mutations, we also evaluated several biomarkers reflecting the mutational status of the patient. We observed a relatively high TMB status in this patient as compared to the clinical cohort, while the MSI status was observed to be non-MSI high for this patient as well as it was stable as most breast cancer patient clinical cohort in general (Fig. 5A and B). We also evaluated chromosomal instability and found that while the fraction genome altered (FGA) and copy number aberration (CNA) scores of the patient lie below or around the lower quartile of the clinical cohort, her copy number heterogeneity (CNH) value is higher than the median of the cohort (Fig. 5C). In addition, we observed several copy-number amplifications in chromosome arms 1q, 6p, 8q, 16p, 19q, 20q (Fig. 5D). Copy-number variations at these chromosome arms have been correlated to poor survival of breast cancer patients [59–63]. TMB represents a predictive biomarker that can be exploited to stratify cancer patients for response to immune checkpoint inhibitor therapies. TMB is indeed believed to be a crucial driver in the generation of immunogenic neopeptides on the tumor cell surface, which can affect the patient response to immune checkpoint inhibitors [64]. Deficiency in the MMR components including MLH1, MSH2, MSH6 and PMS2 along with the presence of immune infiltrate is also a predictive biomarker in guiding the use of immunotherapy [65, 66]. Nevertheless, the analysis of the total number of mutated DDR genes in the breast cancer clinical cohort revealed that the patient harbors less somatic and germline mutations than the other patients (Fig. 5E) predicting still functional DNA damage repair systems.

The spectrum of mutations single base substitution categories (SBS), enriched in C>T, C>A and C>G transitions at trinucleotides is associated with two APOBEC3 (apolipoprotein B mRNA editing enzyme catalytic polypeptide 3) associated signatures (SBS2 and SBS13) (Fig. 5F). The APOBEC3 family of cytidine deaminases provides a defense against viruses by inducing mutations in single-stranded DNA. Of note, APOBEC3 proteins have been associated with increased TMB and genomic instability across different tumor types [67]. Notably, the expression of APOBEC3 proteins is negatively regulated by p53 and TP53 mutations are frequently found in tumors expressing high levels of APOBEC3 [68]. The presence of the p.Arg213stop variant of *TP53* in the patient is therefore consistent with the elevated levels of expression of APOBEC3 transcripts relatively to the clinical cohort (Fig. 5G). However, as already reported for other cases of breast cancer [69], we did not observe a correlation between the enrichment of the APOBEC3 mutational signature and the number of CNA.

Conclusions

Progress has been recently achieved in understanding the genomic diversity of breast cancer, leading to new genome-driven classification of this tumor type into different subtypes, each associated with different clinical outcomes and therapeutic options. Dissecting the gene expression patterns of tumors will substantially help in better understanding breast cancer progression as well as in defining more effective therapeutic strategies. The molecular characterization of this tumor provided several hints indicating poor prognosis with high recurrence probability. The tumor was indeed classified as a claudin-low breast cancer, a subtype of tumors that is generally more aggressive and linked to mesenchymal and stemness features. Deregulation of claudin expression has been indeed implicated in tumor progression, metastasis and chemoresistance in breast cancer.

After surgery, the patient received a first-line chemotherapy treatment which included a combination of adriamycin, cyclophosphamide and paclitaxel, followed by hormone therapy. The patient remained in complete remission so far, but since there are hints for high risk for recurrence, more frequent follow-ups are recommended.

Somatic and germline genetic testing revealed some pathogenic or likely pathogenic variants. We found a pathogenic protein truncating mutation in the *TP53* gene, which is predicted to disrupt its transcriptional activity, and therefore to contribute to chromosomal instability, which might also arise from germline alterations occurring in the DNA repairing genes. The presence of these mutations along with other tumor features suggest the possibility to recommend immunotherapy in case of cancer recurrence. Indeed, the tumor can be classified as a hot tumor because it showed the presence of an abundant immune infiltrate and demonstrated a

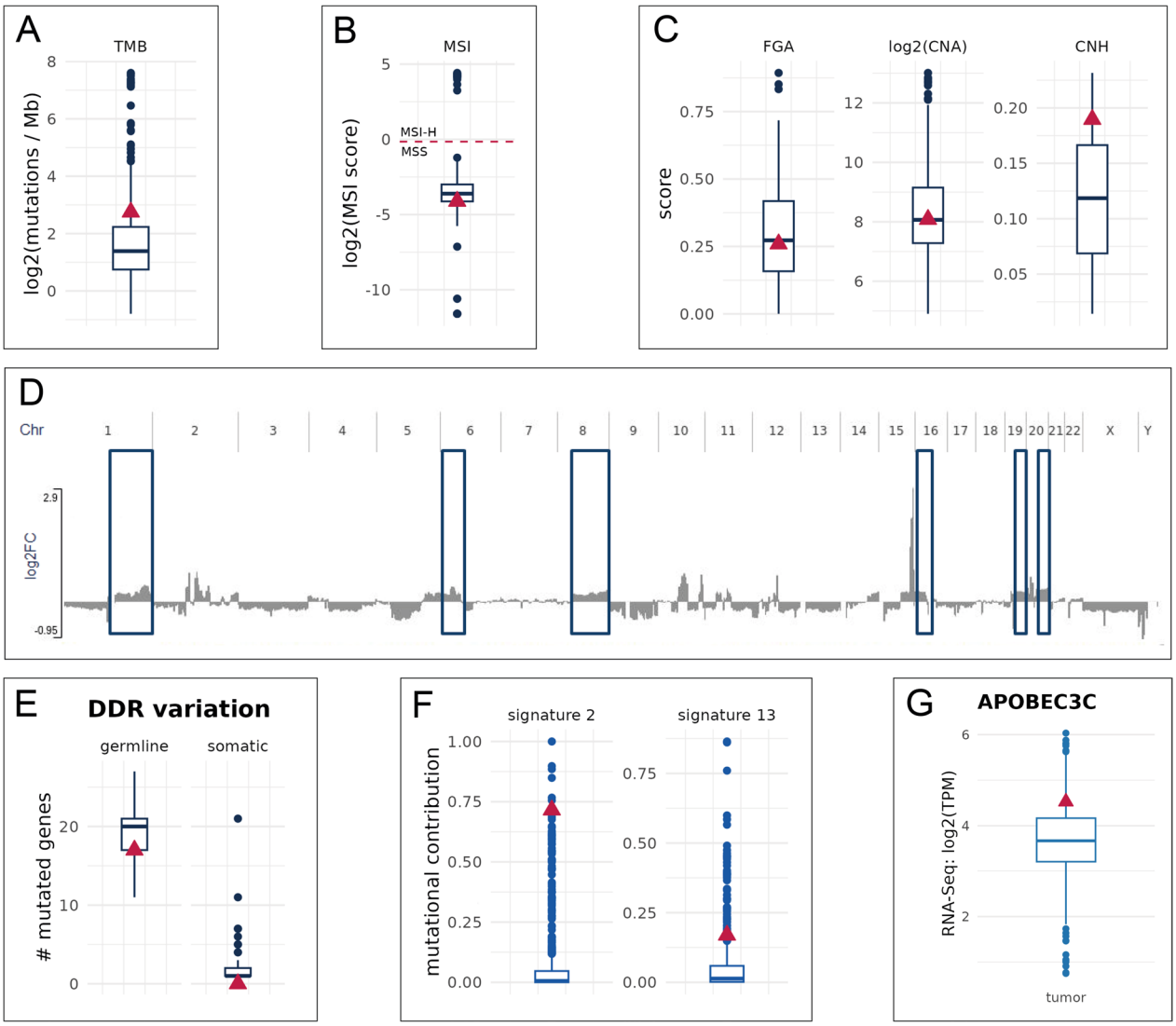

Fig. 5 Evaluation of chromosomal instability in the tumor. **A** TMB status, **B** MSI score, **C** FGA, CNA, and CNH scores, and **D** copy-number variations at chromosome arms 1q, 6p, 8q, 16p, 19q, 20q, **E** total number of mutated DDR genes in the patient. **F** The APOBEC (Ref 2 and Ref13) mutational signatures are enriched in the patient compared to the clinical cohort. **G** RNA-Seq expression levels of APOBEC3C detected in the patient. The patient (red triangle) is compared to the clinical cohort (blue boxplot)

relatively high TMB, thus presenting a promising target for immune checkpoint inhibitor therapy.

Data presented here also indicate the possibility that the patient might acquire endocrine resistance as a result of IGF1R gene amplification and potential activation of the insulin/IGF1 pathway. Indeed, most breast cancer patients progress to endocrine acquired resistance due to the aberrant activation of the insulin/IGF1 signaling pathway.

Materials and methods

Collection of samples

Tumor tissues were globally collected using a standardized protocol, minimizing the ischemia time until freezing in liquid nitrogen. To ensure the quality of the samples, all tissues were hematoxilin- and eosin-stained and subjected to a quality control by a pathologist. Samples needed to be invasive, have a tumor content of $>=30\%$ and necrosis $<=30\%$. Normal tissues were processed in parallel and needed to be free of tumor and representative regarding the tumor tissue to be included [70]. Approximately 10 mg of tissue were taken for

nucleic acid extraction. The remaining tissue was subjected to NGS sequencing [71–73]. To account for tumor heterogeneity, pathological QCs were performed on two sections, before and after taking the analysis material [74–76]. The tissues remained frozen during the entire procedure.

Immunohistochemical analysis

Approximately 1 × 1 × 0.5 cm of tissue was formalin-fixed and paraffin-embedded (FFPE) [77, 78]. Serial sections were used to evaluate prognostic and predictive biomarkers including ER, PR, Ki67, and HER2 through immunohistochemistry [79–81]. Briefly, sections were stained using the automated Leica Bond IHC platform (Leica Biosystems, Deer Park, IL). After antigen retrieval, 4-µm thick sections were incubated with the following primary monoclonal antibodies: mouse monoclonal anti-ER (clone 6F11; Leica Biosystems), mouse monoclonal anti-PR (clone 16; Leica Biosystems), mouse monoclonal anti-Ki67 (clone MM1; Leica Biosystems) and mouse monoclonal anti-HER2 (clone CB11, Leica Biosystems) [82]. Reactions were revealed using BOND-PRIME Polymer DAB Detection System (Leica Biosystems, Deer Park, IL). Immunohistochemistry was evaluated by two blind pathologists in a blinded analysis manner.

Nucleic acid extraction and quality assessment

Frozen tissue slices were mixed with β-mercaptoethanol containing sample buffer and homogenized using the BeadBug system. DNA and RNA were extracted in parallel from the same sample using the Qiagen AllPrep Universal Kit according to the manufacturer's instructions. DNA and RNA concentration were quantified using the Qubit fluorometer with the Qubit dsDNA BR assay or Qubit RNA BR assay respectively. DNA and RNA quality were assessed using the Agilent Tapestation with the Agilent Genomic DNA kit or Agilent High-Sensitivity RNA ScreenTape kit respectively. RNAs need to have a RIN > = 4 or a DV200 > = 60 to be selected for library preparation.

Library preparation and NGS sequencing

Libraries for whole genome sequencing (WGS) were prepared using the PCR-free KAPA Hyper Prep Kit (Roche). For whole transcriptome sequencing, RNA samples were depleted of the ribosomal RNA using the Ribo Zero Kit (Illumina) and library preparation was performed using the TruSeq Stranded Total RNA Kit (Qiagen). All library preparation kits were used according to manufacturer's instructions. Sequencing was performed on a NovaSeq6000 system (Illumina) with paired-end 150 bp sequencing. For WGS, average coverage for tumor samples was > = 60X and > = 30X for normal samples with a total genomic coverage of > = 95%.

Whole transcriptome sequencing datasets have > = 100 million total reads with less than 20% of ribosomal origin and > = 20 million reads mapping to mRNAs according to Ensembl reference. Ribosomal depletion was performed to remove nuclear rRNA and mt-rRNA.

NGS data processing

NGS data was aligned against the GRCh38 genome assembly. Identification and annotation of short genomic variations in normal sample was done using Haplotype Caller (genome analysis toolkit; GATK) [83]. WGS germline variations were called using SnpEff [84] and somatic variations were called using a consensus of Mutect2, Strelka [85], Varscan [86] and Somatic Sniper [87]. Structural variations were called using R packages TitanCNA [88] and DellyCNV [89]. RNA-Seq counts were normalized to transcripts per million (TPM).

Bioinformatical analyses

Mutational signatures were calculated using the R package MutationalPatterns [90]. MSI classification was done using the R package MSIseq [91]. PAM50 subtyping as well as risk scores were investigated using the R package genefu [92]. TMB was calculated as the number of non-synonymous mutations of protein coding genes divided by exome size in Megabases. Pathway analyses were done using R package progeny [93] and immune deconvolution was measured using R package MCPCounter [94]. A combined TCGA-BRCA and METABRIC cohort ($n = 3593$) was analysed to explore the mutational status of the cohort relatively to the patient.

Author contributions

F.B., C.O.B., and E.C. conceived the project, F.B., E.C., J.B., A.M. and G.M. wrote the manuscript, S.G., A.S., L.C., M.S., and V.R. prepared figures. All the Authors have reviewed and approved this submitted version.

Funding

This work has been supported primarily by the MUR-PNRR M4C2I1.3 PE6 project PE00000019 Heal Italia (to EC, GM, FB, AM, SG) and partially by Ministry of Health—HUB LIFE SCIENCE – Advanced Diagnostic- Italian network of excellence for advanced diagnosis (INNOVA) (PNC-E3-2022-23683266) to AM, GM, EC, FB. The Research leading to these results has received funding from Associazione Italiana per la Ricerca contro il Cancro (AIRC) to GM (IG#2022 ID 27366; 2023-2027), to EC (IG#22,206; 2019-2023) and to FB (IG#2019 – 23232). Fondazione Luigi Maria Monti IDI-IRCCS (R.C. to EC). AS was supported by REACT-EU PON "Ricerca e Innovazione 2014-2020" (DM 1062/2021).

Availability of data and materials

Not applicable.

Declarations

Ethics approval and consent to participate

All the procedures carried out in the research with participation of humans were in compliance with the ethical standards of the institutional and/or

national ethics committee and with the Helsinki Declaration of 1964 and its subsequent changes or with comparable ethics standards. Informed voluntary consent was obtained from every participant of the study: approval on 09-2019, number 96-19.

Competing interests
The authors declare no conflict of interest.

Received: 23 April 2024 Accepted: 20 May 2024
Published online: 16 August 2024

References

1. Koboldt DC, Fulton RS, McLellan MD, Schmidt H, Kalicki-Veizer J, McMichael JF, et al. Comprehensive molecular portraits of human breast tumours. Nature. 2012;490:61–70.
2. Yi J, Li H, Chu B, Kon N, Hu X, Hu J, et al. Inhibition of USP7 induces p53-independent tumor growth suppression in triple-negative breast cancers by destabilizing FOXM1. Cell Death Differ. 2023;30:1799–810.
3. Vitale I, Pietrocola F, Guilbaud E, Aaronson SA, Abrams JM, Adam D, et al. Apoptotic cell death in disease—Current understanding of the NCCD 2023. Cell Death Differ. Springer Nature; 2023. p. 1097–154.
4. Saatci O, Akbulut O, Cetin M, Sikirzhytski V, Uner M, Lengerli D, et al. Targeting TACC3 represents a novel vulnerability in highly aggressive breast cancers with centrosome amplification. Cell Death Differ. 2023;30:1305–19.
5. Li J, Dong X, Kong X, Wang Y, Li Y, Tong Y, et al. Circular RNA hsa_circ_0067842 facilitates tumor metastasis and immune escape in breast cancer through HuR/CMTM6/PD-L1 axis. Biol Direct. 2023;18.
6. Kuo WH, Chu PY, Wang CC, Huang PS, Chan SH. MAP7D3, a novel prognostic marker for triple-negative breast cancer, drives cell invasiveness and cancer-initiating cell properties to promote metastatic progression. Biol Direct. 2023;18.
7. Parker JS, Mullins M, Cheang MCU, Leung S, Voduc D, Vickery T, et al. Supervised risk predictor of breast cancer based on intrinsic subtypes. J Clin Oncol. 2023;41:4192–9.
8. Park S, Koo JS, Kim MS, Park HS, Lee JS, Lee JS, et al. Characteristics and outcomes according to molecular subtypes of breast cancer as classified by a panel of four biomarkers using immunohistochemistry. Breast. 2012;21:50–7.
9. Sun G, Wei Y, Zhou B, Wang M, Luan R, Bai Y, et al. BAP18 facilitates CTCF-mediated chromatin accessible to regulate enhancer activity in breast cancer. Cell Death Differ. 2023;30:1260–78.
10. Zhao Y, Huang X, Zhu D, Wei M, Luo J, Yu S, et al. Deubiquitinase OTUD6A promotes breast cancer progression by increasing TopBP1 stability and rendering tumor cells resistant to DNA-damaging therapy. Cell Death Differ. 2022;29:2531–44.
11. Orrantia-Borunda E, Anchondo-Nuñez P, Acuña-Aguilar LE, Gómez-Valles FO, Ramírez-Valdespino CA. Subtypes of Breast Cancer. 2022.
12. Tran B, Bedard PL. Luminal-B breast cancer and novel therapeutic targets. Breast Cancer Res. 2011;13:221.
13. Zhang J, Zhang G, Zhang W, Bai L, Wang L, Li T, et al. Loss of RBMS1 promotes anti-tumor immunity through enabling PD-L1 checkpoint blockade in triple-negative breast cancer. Cell Death Differ. 2022;29:2247–61.
14. Yin X, Teng X, Ma T, Yang T, Zhang J, Huo M, et al. RUNX2 recruits the NuRD(MTA1)/CRL4B complex to promote breast cancer progression and bone metastasis. Cell Death Differ. 2022;29:2203–17.
15. Loibl S, Gianni L. HER2-positive breast cancer. Lancet. 2017;389:2415–29.
16. Collignon J, Lousberg L, Schroeder H, Jerusalem G. Triple-negative breast cancer: treatment challenges and solutions. Breast Cancer (Dove Med Press). 2016;8:93–107.
17. Kuo W-H, Chu P-Y, Wang C-C, Huang P-S, Chan S-H. MAP7D3, a novel prognostic marker for triple-negative breast cancer, drives cell invasiveness and cancer-initiating cell properties to promote metastatic progression. Biol Direct. 2023;18:44.
18. Prat A, Parker JS, Karginova O, Fan C, Livasy C, Herschkowitz JI, et al. Phenotypic and molecular characterization of the claudin-low intrinsic subtype of breast cancer. Breast Cancer Res. 2010;12:R68.
19. Yan Y, He M, Zhao L, Wu H, Zhao Y, Han L, et al. A novel HIF-2α targeted inhibitor suppresses hypoxia-induced breast cancer stemness via SOD2-mtROS-PDI/GPR78-UPRER axis. Cell Death Differ. 2022;29:1769–89.
20. Han X, Ren C, Lu C, Qiao P, Yang T, Yu Z. Deubiquitination of MYC by OTUB1 contributes to HK2 mediated glycolysis and breast tumorigenesis. Cell Death Differ. 2022;29:1864–73.
21. Prat A, Perou CM. Deconstructing the molecular portraits of breast cancer. Mol Oncol. 2011;5:5–23.
22. Dias K, Dvorkin-Gheva A, Hallett RM, Wu Y, Hassell J, Pond GR, et al. Claudin-low breast cancer & clinical & pathological characteristics. PLoS ONE. 2017;12: e0168669.
23. Agostini M, Mancini M, Candi E. Long non-coding RNAs affecting cell metabolism in cancer. Biol Direct. 2022;17:26.
24. Fox EM, Miller TW, Balko JM, Kuba MG, Sánchez V, Smith RA, et al. A kinome-wide screen identifies the insulin/IGF-I receptor pathway as a mechanism of escape from hormone dependence in breast cancer. Cancer Res. 2011;71:6773–84.
25. Marra A, Trapani D, Ferraro E, Curigliano G. Mechanisms of endocrine resistance in hormone receptor-positive breast cancer. Cancer Treat Res. 2023;188:219–35.
26. Galea MH, Blamey RW, Elston CE, Ellis IO. The Nottingham Prognostic Index in primary breast cancer. Breast Cancer Res Treat. 1992;22:207–19.
27. Pommier RM, Sanlaville A, Tonon L, Kielbassa J, Thomas E, Ferrari A, et al. Comprehensive characterization of claudin-low breast tumors reflects the impact of the cell-of-origin on cancer evolution. Nat Commun. 2020;11:3431.
28. Hennessy BT, Gonzalez-Angulo A-M, Stemke-Hale K, Gilcrease MZ, Krishnamurthy S, Lee J-S, et al. Characterization of a naturally occurring breast cancer subset enriched in epithelial-to-mesenchymal transition and stem cell characteristics. Cancer Res. 2009;69:4116–24.
29. Li J, Dong X, Kong X, Wang Y, Li Y, Tong Y, et al. Circular RNA hsa_circ_0067842 facilitates tumor metastasis and immune escape in breast cancer through HuR/CMTM6/PD-L1 axis. Biol Direct. 2023;18:48.
30. Massagué J. TGFbeta in cancer. Cell. 2008;134:215–30.
31. Suriyamurthy S, Baker D, Ten Dijke P, Iyengar PV. Epigenetic reprogramming of TGF-β signaling in breast cancer. Cancers (Basel). 2019;11:726.
32. Padua D, Zhang XH-F, Wang Q, Nadal C, Gerald WL, Gomis RR, et al. TGFbeta primes breast tumors for lung metastasis seeding through angiopoietin-like 4. Cell. 2008;133:66–77.
33. Banerji S, Cibulskis K, Rangel-Escareno C, Brown KK, Carter SL, Frederick AM, et al. Sequence analysis of mutations and translocations across breast cancer subtypes. Nature. 2012;486:405–9.
34. Cancer Genome Atlas Research Network, Weinstein JN, Collisson EA, Mills GB, Shaw KRM, Ozenberger BA, et al. The Cancer Genome Atlas Pan-Cancer analysis project. Nat Genet. 2013;45:1113–20.
35. Paik S, Shak S, Tang G, Kim C, Baker J, Cronin M, et al. A multigene assay to predict recurrence of tamoxifen-treated, node-negative breast cancer. N Engl J Med. 2004;351:2817–26.
36. Pant V, Sun C, Lozano G. Tissue specificity and spatio-temporal dynamics of the p53 transcriptional program. Cell Death Differ. 2023;30:897–905.
37. Panatta E, Butera A, Celardo I, Leist M, Melino G, Amelio I. p53 regulates expression of nuclear envelope components in cancer cells. Biol Direct. 2022;17:38.
38. Butera A, Roy M, Zampieri C, Mammarella E, Panatta E, Melino G, et al. p53-driven lipidome influences non-cell-autonomous lysophospholipids in pancreatic cancer. Biol Direct. 2022;17:6.
39. Cappello A, Tosetti G, Smirnov A, Ganini C, Yang X, Shi Y, et al. p63 orchestrates serine and one carbon metabolism enzymes expression in head and neck cancer. Biol Direct. 2023;18:73.
40. Tatavosian R, Donovan MG, Galbraith MD, Duc HN, Szwarc MM, Joshi MU, et al. Cell differentiation modifies the p53 transcriptional program through a combination of gene silencing and constitutive transactivation. Cell Death Differ. 2023;30:952–65.
41. Li J, Zhan H, Ren Y, Feng M, Wang Q, Jiao Q, et al. Sirtuin 4 activates autophagy and inhibits tumorigenesis by upregulating the p53 signaling pathway. Cell Death Differ. 2023;30:313–26.
42. Smirnov A, Cappello A, Lena AM, Anemona L, Mauriello A, Di Daniele N, et al. ZNF185 is a p53 target gene following DNA damage. Aging. 2018;10:3308–26.
43. Slamon DJ, Leyland-Jones B, Shak S, Fuchs H, Paton V, Bajamonde A, et al. Use of chemotherapy plus a monoclonal antibody against HER2

for metastatic breast cancer that overexpresses HER2. N Engl J Med. 2001;344:783–92.
44. Curtis C, Shah SP, Chin S-F, Turashvili G, Rueda OM, Dunning MJ, et al. The genomic and transcriptomic architecture of 2,000 breast tumours reveals novel subgroups. Nature. 2012;486:346–52.
45. Gao J, Aksoy BA, Dogrusoz U, Dresdner G, Gross B, Sumer SO, et al. Integrative analysis of complex cancer genomics and clinical profiles using the cBioPortal. Sci Signal. 2013;6:pl1.
46. Soni UK, Jenny L, Hegde RS. IGF-1R targeting in cancer - does sub-cellular localization matter? J Exp Clin Cancer Res. 2023;42:273.
47. Farabaugh SM, Boone DN, Lee AV. Role of IGF1R in breast cancer subtypes, stemness, and lineage differentiation. Front Endocrinol (Lausanne). 2015;6:59.
48. Jones RA, Campbell CI, Gunther EJ, Chodosh LA, Petrik JJ, Khokha R, et al. Transgenic overexpression of IGF-IR disrupts mammary ductal morphogenesis and induces tumor formation. Oncogene. 2007;26:1636–44.
49. Schnarr B, Strunz K, Ohsam J, Benner A, Wacker J, Mayer D. Down-regulation of insulin-like growth factor-I receptor and insulin receptor substrate-1 expression in advanced human breast cancer. Int J Cancer. 2000;89:506–13.
50. Hernandez-Boussard T, Rodriguez-Tome P, Montesano R, Hainaut P. IARC p53 mutation database: a relational database to compile and analyze p53 mutations in human tumors and cell lines. International Agency for Research on Cancer. Hum Mutat. 1999;14:1–8.
51. Madorsky Rowdo FP, Xiao G, Khramtsova GF, Nguyen J, Olopade OI, Martini R, et al. Patient-derived tumor organoids with p53 mutations, and not wild-type p53, are sensitive to synergistic combination PARP inhibitor treatment. bioRxiv. 2023;
52. Russo J, Russo IH. Molecular basis of pregnancy-induced breast cancer prevention. Horm Mol Biol Clin Investig. 2012;9:3–10.
53. Rodríguez D, Bretones G, Quesada V, Villamor N, Arango JR, López-Guillermo A, et al. Mutations in CHD2 cause defective association with active chromatin in chronic lymphocytic leukemia. Blood. 2015;126:195–202.
54. Breast Cancer Association Consortium, Dorling L, Carvalho S, Allen J, González-Neira A, Luccarini C, et al. Breast Cancer Risk Genes - Association Analysis in More than 113,000 Women. N Engl J Med. 2021;384:428–39.
55. Worrillow LJ, Travis LB, Smith AG, Rollinson S, Smith AJ, Wild CP, et al. An intron splice acceptor polymorphism in hMSH2 and risk of leukemia after treatment with chemotherapeutic alkylating agents. Clin Cancer Res. 2003;9:3012–20.
56. Wang W-C, Hou T-C, Kuo C-Y, Lai Y-C. Hints from a female patient with breast cancer who later presented with Cowden syndrome. J Breast Cancer. 2020;23:430–7.
57. Santos LS, Silva SN, Gil OM, Ferreira TC, Limbert E, Rueff J. Mismatch repair single nucleotide polymorphisms and thyroid cancer susceptibility. Oncol Lett. 2018;15:6715–26.
58. Jun S-Y, Lee E-J, Kim M-J, Chun SM, Bae YK, Hong SU, et al. Lynch syndrome-related small intestinal adenocarcinomas. Oncotarget. 2017;8:21483–500.
59. Goh JY, Feng M, Wang W, Oguz G, Yatim SMJM, Lee PL, et al. Chromosome 1q21.3 amplification is a trackable biomarker and actionable target for breast cancer recurrence. Nat Med. 2017;23:1319–30.
60. Santos GC, Zielenska M, Prasad M, Squire JA. Chromosome 6p amplification and cancer progression. J Clin Pathol. 2007;60:1–7.
61. Choschzick M, Lassen P, Lebeau A, Marx AH, Terracciano L, Heilenkötter U, et al. Amplification of 8q21 in breast cancer is independent of MYC and associated with poor patient outcome. Mod Pathol. 2010;23:603–10.
62. Lacle MM, Kornegoor R, Moelans CB, Maes-Verschuur AH, van der Pol C, Witkamp AJ, et al. Analysis of copy number changes on chromosome 16q in male breast cancer by multiplex ligation-dependent probe amplification. Mod Pathol. 2013;26:1461–7.
63. Pariyar M, Johns A, Thorne RF, Scott RJ, Avery-Kiejda KA. Copy number variation in triple negative breast cancer samples associated with lymph node metastasis. Neoplasia. 2021;23:743–53.
64. Sha D, Jin Z, Budczies J, Kluck K, Stenzinger A, Sinicrope FA. Tumor mutational burden as a predictive biomarker in solid tumors. Cancer Discov. 2020;10:1808–25.
65. Mestrallet G, Brown M, Bozkus CC, Bhardwaj N. Immune escape and resistance to immunotherapy in mismatch repair deficient tumors. Front Immunol. 2023;14:1210164.
66. Sibilio P, Belardinilli F, Licursi V, Paci P, Giannini G. An integrative in-silico analysis discloses a novel molecular subset of colorectal cancer possibly eligible for immune checkpoint immunotherapy. Biol Direct. 2022;17:10.
67. Jakobsdottir GM, Brewer DS, Cooper C, Green C, Wedge DC. APOBEC3 mutational signatures are associated with extensive and diverse genomic instability across multiple tumour types. BMC Biol. 2022;20:117.
68. Periyasamy M, Singh AK, Gemma C, Kranjec C, Farzan R, Leach DA, et al. p53 controls expression of the DNA deaminase APOBEC3B to limit its potential mutagenic activity in cancer cells. Nucleic Acids Res. 2017;45:11056–69.
69. Roberts SA, Lawrence MS, Klimczak LJ, Grimm SA, Fargo D, Stojanov P, et al. An APOBEC cytidine deaminase mutagenesis pattern is widespread in human cancers. Nat Genet. 2013;45:970–6.
70. Sabelli R, Iorio E, De Martino A, Podo F, Ricci A, Viticchiè G, et al. Rhodanese-thioredoxin system and allyl sulfur compounds. FEBS J. 2008;275:3884–99.
71. Bellomaria A, Barbato G, Melino G, Paci M, Melino S. Recognition mechanism of p63 by the E3 ligase Itch: novel strategy in the study and inhibition of this interaction. Cell Cycle. 2012;11:3638–48.
72. Nepravishta R, Sabelli R, Iorio E, Micheli L, Paci M, Melino S. Oxidative species and S-glutathionyl conjugates in the apoptosis induction by allyl thiosulfate. FEBS J. 2012;279:154–67.
73. Aceto A, Dragani B, Melino S, Allocati N, Masulli M, Di Ilio C, et al. Identification of an N-capping box that affects the alpha 6-helix propensity in glutathione S-transferase superfamily proteins: a role for an invariant aspartic residue. Biochem J. 1997;322(Pt 1):229–34.
74. Fazi B, Melino S, De Rubeis S, Bagni C, Paci M, Piacentini M, et al. Acetylation of RTN-1C regulates the induction of ER stress by the inhibition of HDAC activity in neuroectodermal tumors. Oncogene. 2009;28:3814–24.
75. Melino S, Leo S, Toska PV. Natural hydrogen sulfide donors from Allium sp. as a nutraceutical approach in Type 2 diabetes prevention and therapy. Nutrients. 2019;11:1581.
76. Melino S, Paci M. Progress for dengue virus diseases. Towards the NS2B-NS3pro inhibition for a therapeutic-based approach. FEBS J. 2007;274:2986–3002.
77. Scimeca M, Anemona L, Granaglia A, Bonfiglio R, Urbano N, Toschi N, et al. Plaque calcification is driven by different mechanisms of mineralization associated with specific cardiovascular risk factors. Nutr Metab Cardiovasc Dis. 2019;29:1330–6.
78. Scimeca M, Giocondo R, Montanaro M, Granaglia A, Bonfiglio R, Tancredi V, et al. BMP-2 variants in breast epithelial to mesenchymal transition and microcalcifications origin. Cells. 2020;9:1381.
79. Bonfiglio R, Milano F, Cranga A, De Caro MT, Kaur Lamsira H, Trivigno D, et al. Negative prognostic value of intra-ductal fat infiltrate in breast cancer. Pathol Res Pract. 2019;215: 152634.
80. Scimeca M, Bonfiglio R, Menichini E, Albonici L, Urbano N, De Caro MT, et al. Microcalcifications drive breast cancer occurrence and development by macrophage-mediated epithelial to mesenchymal transition. Int J Mol Sci. 2019;20:5633.
81. Vitali A, Botta B, Delle Monache G, Zappitelli S, Ricciardi P, Melino S, et al. Purification and partial characterization of a peroxidase from plant cell cultures of *Cassia didymobotrya* and biotransformation studies. Biochem J. 1998;331(Pt 2):513–9.
82. Sunzini F, De Stefano S, Chimenti MS, Melino S. hydrogen sulfide as potential regulatory gasotransmitter in arthritic diseases. Int J Mol Sci. 2020;21:1180.
83. McKenna A, Hanna M, Banks E, Sivachenko A, Cibulskis K, Kernytsky A, et al. The genome analysis toolkit: a MapReduce framework for analyzing next-generation DNA sequencing data. Genome Res. 2010;20:1297–303.
84. Cingolani P, Platts A, Wang LL, Coon M, Nguyen T, Wang L, et al. A program for annotating and predicting the effects of single nucleotide polymorphisms, SnpEff: SNPs in the genome of Drosophila melanogaster strain w1118; iso-2; iso-3. Fly (Austin). 2012;6:80–92.
85. Kim S, Scheffler K, Halpern AL, Bekritsky MA, Noh E, Källberg M, et al. Strelka2: fast and accurate calling of germline and somatic variants. Nat Methods. 2018;15:591–4.
86. Koboldt DC, Chen K, Wylie T, Larson DE, McLellan MD, Mardis ER, et al. VarScan: variant detection in massively parallel sequencing of individual and pooled samples. Bioinformatics. 2009;25:2283–5.

87. Larson DE, Harris CC, Chen K, Koboldt DC, Abbott TE, Dooling DJ, et al. SomaticSniper: identification of somatic point mutations in whole genome sequencing data. Bioinformatics. 2012;28:311–7.
88. Ha G, Roth A, Khattra J, Ho J, Yap D, Prentice LM, et al. TITAN: inference of copy number architectures in clonal cell populations from tumor whole-genome sequence data. Genome Res. 2014;24:1881–93.
89. Rausch T, Zichner T, Schlattl A, Stütz AM, Benes V, Korbel JO. DELLY: structural variant discovery by integrated paired-end and split-read analysis. Bioinformatics. 2012;28:i333–9.
90. Manders F, Brandsma AM, de Kanter J, Verheul M, Oka R, van Roosmalen MJ, et al. MutationalPatterns: the one stop shop for the analysis of mutational processes. BMC Genom. 2022;23:134.
91. Bonneville R, Krook MA, Kautto EA, Miya J, Wing MR, Chen H-Z, et al. Landscape of microsatellite instability across 39 cancer types. JCO Precis Oncol. 2017;2017:1.
92. Huang MN, McPherson JR, Cutcutache I, Teh BT, Tan P, Rozen SG. MSIseq: software for assessing microsatellite instability from catalogs of somatic mutations. Sci Rep. 2015;5:13321.
93. Schubert M, Klinger B, Klünemann M, Sieber A, Uhlitz F, Sauer S, et al. Perturbation-response genes reveal signaling footprints in cancer gene expression. Nat Commun. 2018;9.
94. Becht E, Giraldo NA, Lacroix L, Buttard B, Elarouci N, Petitprez F, et al. Estimating the population abundance of tissue-infiltrating immune and stromal cell populations using gene expression. Genome Biol. 2016;17.

Publisher's Note